Effects of miR-939 and miR-376A on ulcerative colitis using a decoy strategy to inhibit NF-κB and NFAT expression

Yongwei Lin,[1]* Zhipeng Zhou,[1]* Lang Xie,[1] Yongsheng Huang,[1] Zhenghua Qiu,[1] Lili Ye,[2] Chunhui Cui[1]

[1]Department of General Surgery
[2]Department of Neurosurgery, Zhujiang Hospital, Southern Medical University, Guangzhou, China
**These authors contributed equally to this study*

ABSTRACT

The aim of this study was to explore the effects of miR-939 and miR-376A on the pathogenesis of ulcerative colitis (UC) by using a decoy strategy to regulate the expression of nuclear transcription factor kappa B (NF-κB) and nuclear factor of activated T cells (NFAT). Such strategies represent a potential novel treatment for UC. Quantitative polymerase chain reaction (qPCR) analysis was used to detect the differences between the expression of miR-939, miR-376a, NF-κB, NFAT in the tissue samples from the resting and active stages of UC and healthy controls, and analyzed the correlation. The electrophoretic mobility shift assay was used to validate the ability of miRNAs to bind to NF-κB and NFAT. The expression of components of the intestinal barrier in UC and changes in apoptosis-related factors were examined by Western blotting, qPCR, and immunofluorescence. After a dextran sulfate sodium (DSS)-induced mouse model of UC was established, the morphological changes in the colonic tissues of mice, the changes in serum inflammatory factors, and the changes in urine protein or urine leukocytes, liver enzymes, and prothrombin time were measured to examine intestinal permeability. The expression of miR-939 and miR-376a in human UC tissue was significantly lower than that in the normal control tissue, and was negatively correlated with the expression of NF-κB and NFAT. miR-939 and miR-376a decoy strategies resulted in a beneficial increase in the expression of claudins, occludins, and ZO-1 protein and inhibited apoptosis in intestinal epithelial cells. The disease activity index of the UC model group was significantly higher than that of the normal control group. The expression of inflammatory factors in the decoy group was higher than that in the UC model group. Therefore, from the experimental results, it can be concluded that using miR-939 and miR-376a to trap NF-κB and NFAT inhibits the activation of transcription factors NF-κB and NFAT, which in turn inhibits the expression of inflammatory factors and results in partial recovery of the intestinal barrier in UC. The decoy strategy inhibited apoptosis in the target cells and had a therapeutic effect in the mice model of UC. This study provides new ideas for the development of future clinical therapies for UC.

Key words: miR-939; miR-376A; NF-κB; NFAT; decoy strategy; ulcerative colitis.

Correspondence: Chunhui Cui, Department of General Surgery, Zhujiang Hospital, Southern Medical University, Guangzhou 510282, China. E-mail: drcuich@163.com

Contribution: LY, CC, conceived the study and designed the experiments; YL, ZZ, completed the experiment, analyzed the data and wrote the manuscript; LX, YH, ZQ, discussed the results and revised the manuscript. All the authors have read and approved the final version of the manuscript and agreed to be accountable for all aspects of the work.

Conflict of interest: The authors declare that they have no competing interests, and all authors confirm accuracy.

Availability of data and materials: The datasets used and/or analyzed during the current study are available from the corresponding author on reasonable request.

Ethical approval: Ethical approval was obtained for all experimental procedures by the Ethics Committee of the Zhujiang Hospital, Southern Medical University, Guangzhou, China.

Patient consent for publication: Verbal informed consent was obtained from the patients for their anonymized information to be published in this article.

Introduction

Ulcerative colitis (UC) is the occurrence of chronic, non-specific inflammatory lesions mainly in the colorectal mucosa and submucosa, and presents as intestinal mucosal hyperemia, erosion, ulcers, and hyperplasia.[1,2] Studies in developed Western Countries, such as the United States, have revealed an annual incidence rate of approximately 2-10 individuals per 10 million, and that the number of cases reported in the past decade is 3.8 times higher than that in the preceding decade. The incidence in China and some Asian Countries is also increasing annually.[3,4] Owing to the complex etiology of UC and the coexistence of multiple pathogenesis, clinical treatment is often limited to only a single mechanism treatment; consequently, the clinical efficacy is not obvious, the disease is difficult to cure, and recurrence is often a problem.[5,6]

Transcription factors (TFs) control almost all cell differentiation and organ formation, cell growth and apoptosis, and cell signal transduction through the transcriptional regulation of gene expression.[7,8] TFs include nuclear transcription factor kappa B (NF-κB) and nuclear factor of activated T cells (NFAT). NF-κB, as a pivot in the signal transduction pathway, plays a key regulatory role in cytokine-induced gene expression, and participates in various biological processes, such as immune response, the inflammatory response, apoptosis, and tumorigenesis.[9-11]

In recent years, decoy strategies have been widely studied and applied to explore the function of TFs.[12] A synthetic double-chain oligodeoxynucleotide (ODN) fragment containing the binding site sequence of a transcription factor can compete with the normal binding site of the transcription factor and block the activity of the transcription factor. In recent years, there have been many reports on the use of decoy strategies to study TFs, including NF-κB, Sp1, and NFAT.[13,14]

MicroRNAs (miRNAs) have been reported to produce the post-transcriptional inhibition of gene expression.[15] Moreover, decoy ODN and miRNA have a similar double-stranded structure, and some researchers have proposed that miRNA may act as an endogenous decoy molecule that causes the transcriptional regulation of gene expression.[16] It has been demonstrated that miR-939 and miR-376a bind to the TFs NF-κB and NFAT, and that Bcl-XL and FasL/miR-26, as the transcriptional targets of NF-κB and NFAT, can be regulated by miR-939 and miR-376a. Therefore, this scholar proved that these miRNAs can indeed act as decoy molecules to regulate the transcriptional activity of TFs.[16] NF-κB and NFAT can regulate the proliferation and differentiation of T cells and participate in the immune regulation of the intestinal inflammatory system.[17,18] Therefore, the inhibition of NF-κB and NFAT transcriptional activity is important for the treatment of colitis. To achieve this, miR-939 and miR-376a were selected as endogenous decoy molecules for NF-κB and NFAT.

In this study, we hypothesized that miR-939 and miR-376A could regulate the expression of NF-κB and NFAT through a decoy strategy to regulate the pathogenesis of UC. miR-939 and miR-376a decoy ODNs were designed, transfected into intestinal epithelial cells in conjunction with NF-κB and NFAT, and the expression of TFs, inflammatory factors, and apoptosis-related proteins was detected. A DSS-induced mouse model of UC was established to analyze the effects of miR-939 and miR-376a on the pathogenesis of UC. This study not only supplements the theoretical exploration of the mechanism of UC pathogenesis, but also provides new ideas for the development of future clinical therapies for UC.

Materials and Methods

Cell culture

Clinical samples were collected from patients with UC referred to the Zhujiang Hospital, Southern Medical University, Guangzhou (China): the diagnosis of UC complied with the 2004 American Gastroenterological Association adult UC practice guideline[19] and the 2010 consensus opinion on the diagnosis and treatment of inflammatory bowel disease in China.[20] The obtained colon tissue was placed in a sterile petri dish and washed several times with phosphate-buffered saline (PBS) solution. The tissue was cut into pieces, put into a centrifuge tube, and PBS solution was added for repeated blowing and washing. The mixed digestion liquid was added to the tissue and it was placed in a 37°C water bath and left to shake for 30 min. After standing for 1 min, the supernatant was transferred to another centrifuge tube. The culture solution was added and the digestion steps were repeated 2 or 3 times. The supernatant was collected and centrifuged at 1000 r/min for 5 min. The supernatant was added to the culture medium, blown, mixed, and centrifuged. After the centrifugation step was repeated 5-6 times, the precipitates were directly cultured in RPMI 1640 medium containing 20% fetal bovine serum, and then cultured in an incubator at 37°C containing 5% CO_2. Another section of the colon tissue was placed in liquid paraffin, cooled, embedded, and refrigerated until use. For analysis, the embedded tissue was removed from the refrigerator and sliced.

In situ hybridization

Pepsin hydrochloric acid mixture (0.8%) was added to the slides, which were then digested at 37°C in a water bath for 10 min, washed three times with TBS, dehydrated in a gradient ethanol series, and dried at 20°C. The fluorescence probes were added to the slices, covered by a coverslip, denatured at 98°C for 10 min, annealed in an ice bath, hybridized at 37°C in a water bath for 60 min, washed three times with TBS, and alkaline phosphatase-labeled digoxin antibody was added (Bersinbio, Guangzhou, China). After the slides were left to stand at room temperature for 30 min, they were washed twice with a special washing solution, BCIP/NBT was added for color development, and the slides were left to stand in the dark. After the color development was terminated, 0.3% nuclear Fast Red was used to stain the epithelial cell lining, dehydrated, and sealed with a transparent seal. *In situ* hybridization was used to analyze the expression of miR-939, miR-376, NF-κB, and NFAT in patient samples and healthy controls, and to determine potential correlations.

Synthesis of ODN and selection of target sequences

The mutants of miR-376 and miR-939, antisense oligonucleotide inhibitors against miR-939 and miR-376, were synthesized. NF-κB and NFAT promoter-luciferase fusion plasmids were established. To prepare decoy ODN, the NF-κB decoy ODN and NFAT decoy ODN were designed based on the NF-κB element or NFAT element of c-myc gene promoter region, respectively. The sequences used for the NF-κB decoy ODN were: 5'-GAGUGGGACTTTCCCAGCGTG-3' (sense), 5'-CTCGCTGGGAAAGTCCCACTC-3' (antisense), and the sequences used for the NFAT decoy ODN were: 5'-CGCCCAAA-GAGGAAAATTTGTTTCATA-3' (sense), 5'-TATGAAA-CAAATTTCCTCTTTGGGCG-3' (antisense). As stated in the literature, TNF-a is a proinflammatory cytokine, and the stimulation of HT29 cells with TNF-a can be used to simulate an in vitro cell model of UC.[21] NF-κB decoy and NFAT decoy ODNs were transfected into model cells using the Lipofectamine 2000. After 48 h, the luciferase activity was measured to analyze the transfection efficiency.

Electrophoretic mobility shift assay

The cultured cells were lysed, placed in an ice bath for 30 min, and the nuclear proteins were extracted by centrifugation. The EMSA/Gel-Shift kit (Beyotime, Shanghai, China) was used to configure the oligonucleotide probe reaction system for the target genes. The antibody was mixed with nuclear protein extract and left to stand at 37°C for 2 h. After binding buffer was added, the tubes were incubated at 37°C for 10 min. Finally, labeled probe was added to each tube, and the tubes were incubated for 20 min. The proteins were resolved by gel electrophoresis.

ELISA

The abovementioned model cells were seeded in 100-mm culture plates and left to adhere. The complete growth medium was then removed and the cells were washed three times with PBS. Subsequently, 10 mL of fresh serum-free basal medium was added and the cells were incubated at 37°C in 5% CO_2 for 3 days. The medium was collected and centrifuged at 3,000 rpm for 15 min and 4°C. The culture supernatant was collected, and the secretion of IL-8, IL1b, IL2, G-CSF, GM-CSF, and MIP-2α was detected using ELISA kits (R&D Systems Europe, Abingdon, UK) in accordance with the manufacturer's protocol. The effects of different treatments on UC cell inflammatory factors were detected. The absorbance at 450 nm was detected using a microplate reader (Synergy H1 M; Biotek, Winooski, VT, USA). At least three separate culture plats were assayed for each clone.

Western blotting assay

The cells in each group were collected and the lysate was added to extract the total protein. The proteins were isolated by gel electrophoresis, transferred to a cellulose membrane, and sealed with blocking solution for 2 h. The primary antibody solution (Abcam, Cambridge, UK) was added and incubated at 4°C overnight. TBST solution was added the membranes were washed three times. Then, HRP-conjugated secondary antibody (Abcam, 1:2000 dilution) was added and incubated at room temperature for 30 min. After three washes in TBST solution, the chromogenic ECL agent was added. After 1 min, a chemiluminescence imaging system was used to detect the exposure of the target band. The primary antibodies and dilutions used in the experiment were: anti-TNF-α (1:1000), anti-TLR4 (1:2000), anti-claudin (1:1000), anti-occludin (1:1000), anti-ZO-1 (1:1000), anti-XIAP antibody (1:5000), anti-cIAP (1:1000), anti-Bax (1:500), and anti-caspase-3 (1:1000).

RT-PCR

The cells were inoculated into 96-well plates, and Trizol was added into each well to extract the total RNA. MMLV was used to reverse-transcribe cDNA and the concentration of DNA was detected. The primers for miR-939 and miR-376a were constructed using cDNA as template, and a TaqMan probe set for Muc5ac (Mm01276718-m1; Applied Biosystems, Foster City, CA, USA), and real-time PCR Master Mix (Toyobo Biotech, Osaka, Japan) with a Prism 7900HT Real-Time PCR System (Applied Biosystems) were used to detect the target genes. GAPDH was used as an internal reference. The mRNA expression of miR-939 and miR-376a was detected by RT-PCR. The PCR cycle conditions were: 94°C for 60 s, 37°C for 60 s, and 72°C for 2 min, and 28 cycles were used.

Immunohistochemical studies

Immunohistochemical staining was performed using the immunoperoxidase avidin-biotin complex method (Vectastain Elite ABC kit). Immune complexes were stained using 0.05% 3,3'-diaminobenzidine, and the slides were counterstained with hematoxylin. Paraffin sections were stained with rabbit anti-NF-κB antibody (1:500; Bioworld Technology, St Louis Park, MN, USA) and incubated overnight at 4°C, while the negative control group was cultured with the same dose of PBS solution. On the second day, slice with rabbit anti-NFAT antibody (1:500, Affinity) and react at room temperature for 30 min. All antibodies were diluted with PBS solution. These results were combined with pathological data to analyze the correlation between miR-939 and NF-κB, and miR-376 and NFAT.

Cytometry

Flow cytometry was used to detect the transfected model cells. Transfected cells were collected, washed and resuspended with 1×binding buffer. FITC-Annexin V solution and PI solution were added into cell suspension and stained at room temperature for 15 min under dark conditions. Flow cytometry (Beckman Coulter, Jangsu, China) was used to detect the early apoptosis and late apoptosis rate of stained cells.

Animal experiment

The mice used in this experiment were obtained from Wuhan Biofavor Biotechnology Service Co., Ltd. The experiments were approved by the Ethics Committee of Zhujiang Hospital of Southern Medical University. Twenty-four SD rats were randomly divided into the normal control group (6 rats) and the UC model group (18 rats). DSS was dissolved in distilled water to prepare a 5% DSS (w/w) solution, which was supplied freely to the rats as drinking water. The UC model (18 rats) was randomly divided into the transfection artificial decoy group (6 rats), the miRNA-decoy ODN group (6 rats), and the normal saline group. The artificial decoy (NF-κB, NFAT) and miRNA-decoy (−939, −376A) ODNs were injected into the colon, successively. The method of administration, time, dose, and frequency used in this study were determined from previous studies.[11] At 6 h after successful transfection, fluorescein isothiocyanate[16] was used to detect the permeability of the intestinal tract *in vivo*. The white blood cell (WBC) count, prothrombin time, blood urea nitrogen (BUN), creatinine (CREA), glutamic (GLU), alanine transaminase (ALT), and aspartate transaminase (AST) concentrations were measured at 12 and 24 h after transfection, and changes in indicators, such as urine protein or urine leukocytes, were analyzed at 24 h after transfection. At 24, 48, and 72 h after transfection, the left colon of each rat was taken for gross observation and hematoxylin and eosin (HE) staining to observe the morphological changes of colon tissue, and immunohistochemical staining was used to observe the expression of NF-kBp65 in colonic mucosal cells. Primary abdominal intestinal epithelial cells were isolated, and the expression of apoptosis-related proteins (cIAP, XIAP, Bax, caspase-3, and claudin) was detected.

Statistical analysis

All statistical analyses were calculated using SPSS software (version 20.0 J, SPSS Inc., Chicago, IL, USA), with p-values <0.05 considered statistically significant. Count data were compared using the χ^2-test, whereas continuous variables, which were reported as the mean ± standard deviation were compared using Student's *t*-test. All experiments were repeated three times.

Results

Expression of miR-939 and miR-376A in patients with UC

The expression of miR-939 and miR-376A in tissues from

patients with UC was significantly lower than that in normal human tissues (Figure 1A). The results of WB detection showed that the expression of NF-κB and NFAT in UC tissues was significantly higher than that in normal human tissues (Figure 1B). The expression of miR-939, miR-376A, NF-κB, and NFAT were negatively correlated in patients with UC and healthy controls.

The use of miR-939 and miR-376A to trap NF-κB and NFAT and analysis of their influence on the expression of inflammatory factors

NF-κB decoy ODNs and NFAT decoy ODNs were transfected into TNF-α-stimulated HT29 cells. After 48 h, compared with the control group, the miR-939 antisense oligonucleotide inhibitor group, and the miR-376 antisense oligonucleotide inhibitor group, the luciferase activity of the NF-κB decoy ODN group and the NFAT decoy ODN group was significantly reduced (Figure 2A); the secretion of IL-8, IL1b, IL2, G-CSF, GM-CSF, and MIP-2α was significantly decreased; and the secretion of TNF-a and TLR4 was statistically significantly decreased (Figure 2 B,C) ($p<0.05$). However, when comparing the miR-939 and miR-376 groups with the NF-κB decoy ODN group and NFAT decoy ODN group, no significant differences were found ($p>0.05$).

Effects of miR-939 and miR-376A decoy strategies on the intestinal barrier tight junction and permeability restoration in UC

miR-939, miR-376A, and decoy ODNs were transfected into the intestinal epithelial cells. Immunofluorescence staining of the intestinal epithelial tight junction proteins claudins, occludins, and ZO-1 was performed. Laser confocal microscopy imaging found that the distribution of claudins, occludins, and ZO-1 was not significantly altered in the miR-939 group and the decoy ODN group, but that it was significantly different in the miR-939 antisense oligonucleotide inhibitor group. There was no significant difference in the distribution of claudins, occludins, and ZO-1 in the miR-939 group and the decoy ODN group, but that it was significantly different in the miR-376a antisense oligonucleotide inhibitor group (Figure 3A).

The Western blotting analysis showed that the expression levels of claudins, occludins, and ZO-1 in the miR-939 and decoy ODN groups were significantly higher than those in the miR-939 antisense oligonucleotide inhibitor group and the control group, and that the decoy strategy resulted in the restoration of claudins, occludins, and ZO-1 protein levels (Figure 3B).

The RT-PCR analysis showed that the mRNA expression of claudins, occludins, and ZO-1 in the miR-939 and decoy ODN groups was significantly higher than those in the miR-939 antisense oligonucleotide inhibitor group and the control group, and the decoy strategy was beneficial for recovery of the mRNA expression claudins, occludins, and ZO-1 mRNA (Figure 3C).

Inhibitory effect of trap strategy on intestinal epithelial cell apoptosis

miR-939 and miR-376A and decoy ODNs were transfected into intestinal epithelial cells. The Western blotting analysis showed that the expression levels of cIAP and XIAP proteins in the miR-939 group and the decoy ODN group were lower than those in the miR-939 antisense oligonucleotide inhibitor group. The antisense oligonucleotide inhibitor group and control group were significantly increased. The levels of Bax and Caspase-3 proteins in the miR-939 group and decoy ODN group were higher than those in the miR-939 antisense oligonucleotide inhibitor group. The levels were significantly reduced in the antisense oligonucleotide inhibitor group and the control group, and the decoy strategy resulted in the inhibition of apoptosis in intestinal epithelial cells (Figure 4 A,B). Flow cytometry was used to analyze the transfected model cells. The proportion of apoptotic cells was significantly lower in the miR-939 and decoy ODN groups than in the miR-939

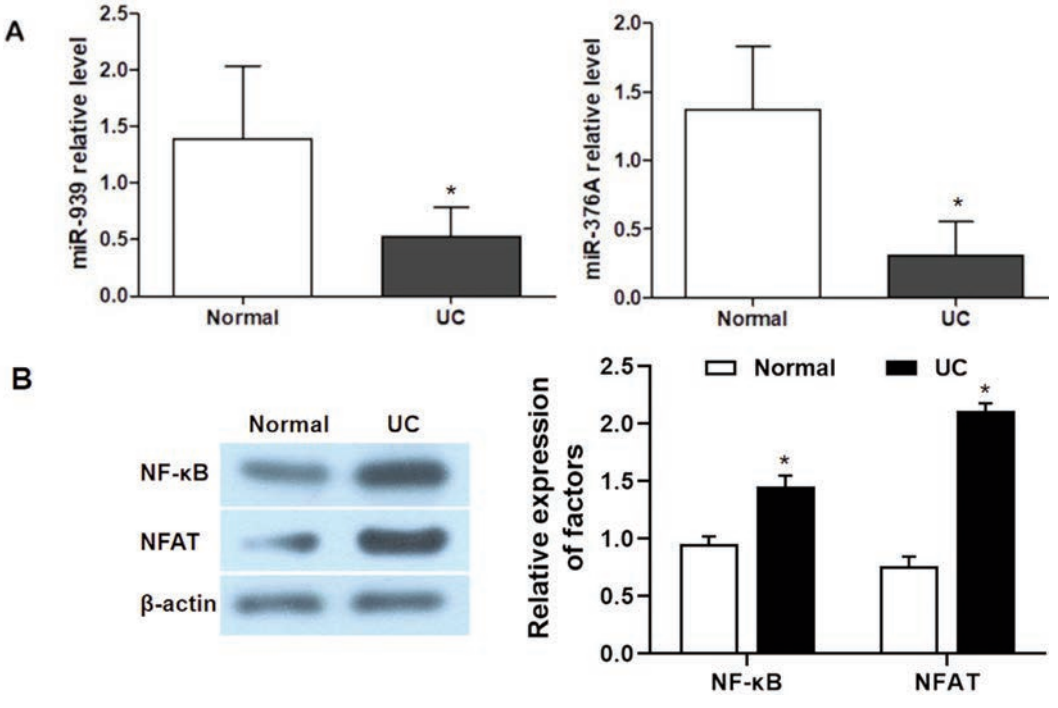

Figure 1. Expression of miR-939, miR-376a, NF-κB, and NFAT in UC patients. A) The expression of miR-939 and miR-376a in UC patient tissues and normal human tissues. B) The expressions of NF-κB and NFAT in UC patient tissues and normal human tissues. Compared with normal group; *p<0.05.

antisense oligonucleotide inhibitor group and control group (Figure 4C). Thus, the trap strategy inhibited apoptosis of intestinal epithelial cells.

Therapeutic effects and side effects of trapping strategies in a mouse model of UC

SD rats were randomly divided into the normal control group (6 rats) and the UC model group (18 rats). The disease activity index of the UC model group was statistically significantly higher than that of normal control group ($p<0.05$).

At 6 h after successful transfection, the permeability of the living intestinal cells was detected. The intestinal permeability of the artificial decoy group and the transfected miRNA-decoy ODN group was significantly lower than that of the UC model group (Figure 5A).

At 24 h after transfection, compared with the UC model group, the WBC count, BUN, Glu, ALT, AST, and 24 h urinary protein content in serum were lower in the artificial mutagenation group and miRNA-mutagenated ODN group, whereas the APTT, PT, and CRAE contents were higher. The same results were found after transfection for 48 h.

At 24, 48, and 72 h after transfection, the staining intensity of NF-kB p65 in colonic mucosal cells was significantly higher in the artificial decoy group and the transfected miRNA-decoy ODN group than in the UC model group (Figure 5 B,C). The expression levels of apoptosis-related protein Bax and Caspase 3 in the miRNA-decoy ODN group and normal control group were significantly lower than those in the UC group. The expression levels of cIAP, XIAP and claudins in the artificial decoy group and the transfected miRNA-decoy ODN histones were statistically significantly higher than those in the normal control group ($p<0.05$) (Figure 5D).

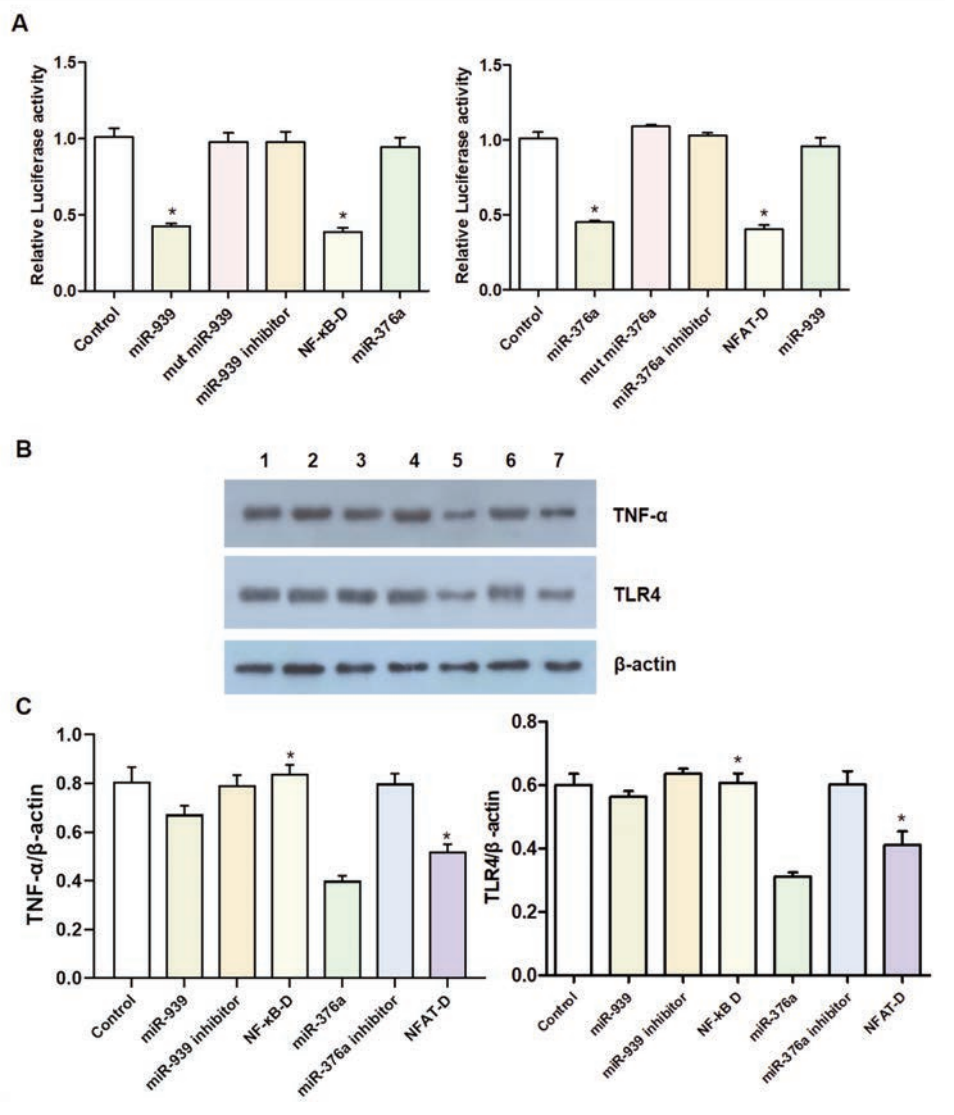

Figure 2. MiR-939 and miR-376a were used to trap NF-κB and NFAT: analyze of their influence on the expression of inflammatory factors. A) The effects of NF-κB decoy ODNs and NFAT decoy ODNs transfection on luciferase activity in different treatment groups were detected by luciferase reporter gene assay. B,C) The expression of TNF-α and TLR4 was detected by Western blotting. Compared with control group, miR-939 antisense oligonucleotide inhibitor group, and miR-376 antisense oligonucleotide inhibitor group; *p<0.05.

Discussion

Impaired intestinal mucosal barrier function is a key element of the occurrence and development of UC.[22] The intestinal mucosal barrier consists of the tight junction protein claudin between adjacent epithelial cells. Previous studies[23,24] found that the expression of claudin-1, -3, -4, -5 is downregulated in the acute phase of UC. Therefore, changes in the distribution structure of claudin protein directly affect its closely linked structure and function, and the detection of claudin can be used to observe changes in the function of cells in UC. Intestinal epithelial cell apoptosis is an important manifestation of the occurrence and development of UC. Some studies have shown that certain inflammatory cytokines can prevent apoptosis in intestinal epithelial cells during the treatment of UC.[25] Therefore, reversing the process of apoptosis through various pathways is essential for the treatment of UC. It is generally

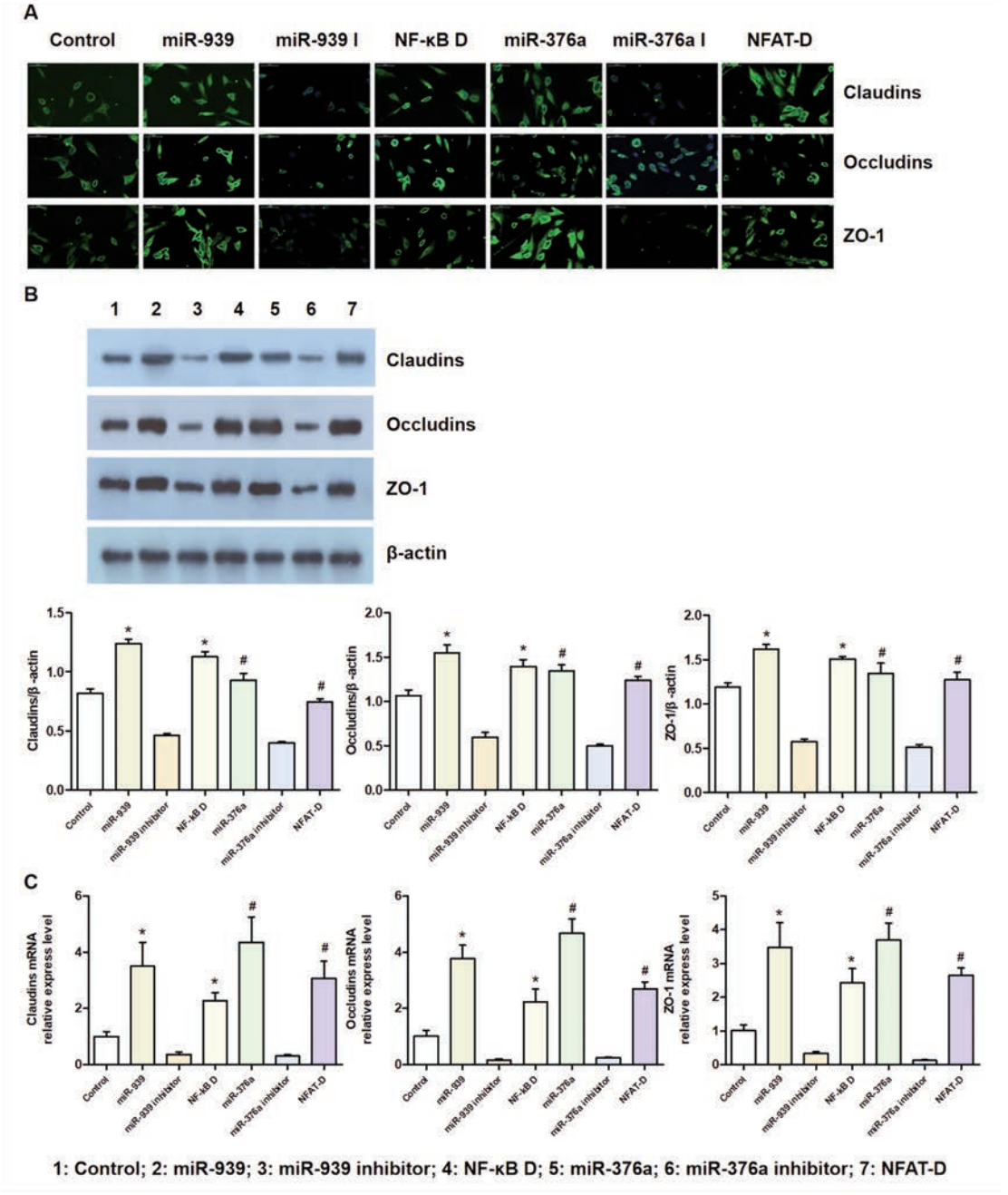

Figure 3. Analysis of the decoy strategy's effect on the tight connection and permeability restoration of intestinal barrier in UC. A) The distribution of claudins, occludins, and ZO-1 in cells was detected by immunofluorescence. B) The protein expression levels of claudins, occludins, and ZO-1 were detected by Western blot. C) The mRNA expression levels of claudins, occludins, and ZO-1 was detected by RT-PCR. Compared with control group, and miR-939 antisense oligonucleotide inhibitor group, *p<0.05; compared with control group, and miR-376a antisense oligonucleotide inhibitor group, #p<0.05.

believed that the pathogenesis of UC is closely related to autoimmune damage and inflammatory infection. There is sufficient evidence[26] that in patients with UC, bacteria can activate the related transcription genes to promote the production of regulatory cytokines, such as TNF-a and CD8-T, by immune-active Th1 and 2 cells.[27]

The results of this study showed that the expression of miR-939 and miR-376A in tissues from patients with UC was significantly lower than that in healthy human tissues. There was a negative correlation of the expression of miR-939, miR-376a, NF-κB, and NFAT between healthy subjects and patients with UC. After transfection of the UC model cells for 48 h, the luciferase activity of the NF-κB bait ODN group and the NFAT bait ODN group was significantly lower than that in the other groups, and the expression of related inflammatory factors was significantly lower. Binding sites have been identified between miR-939 and NF-κB, and miR-376a and NFAT, which demonstrated that miR-939 and miR-376a were potential decoy molecules that could regulate the expression

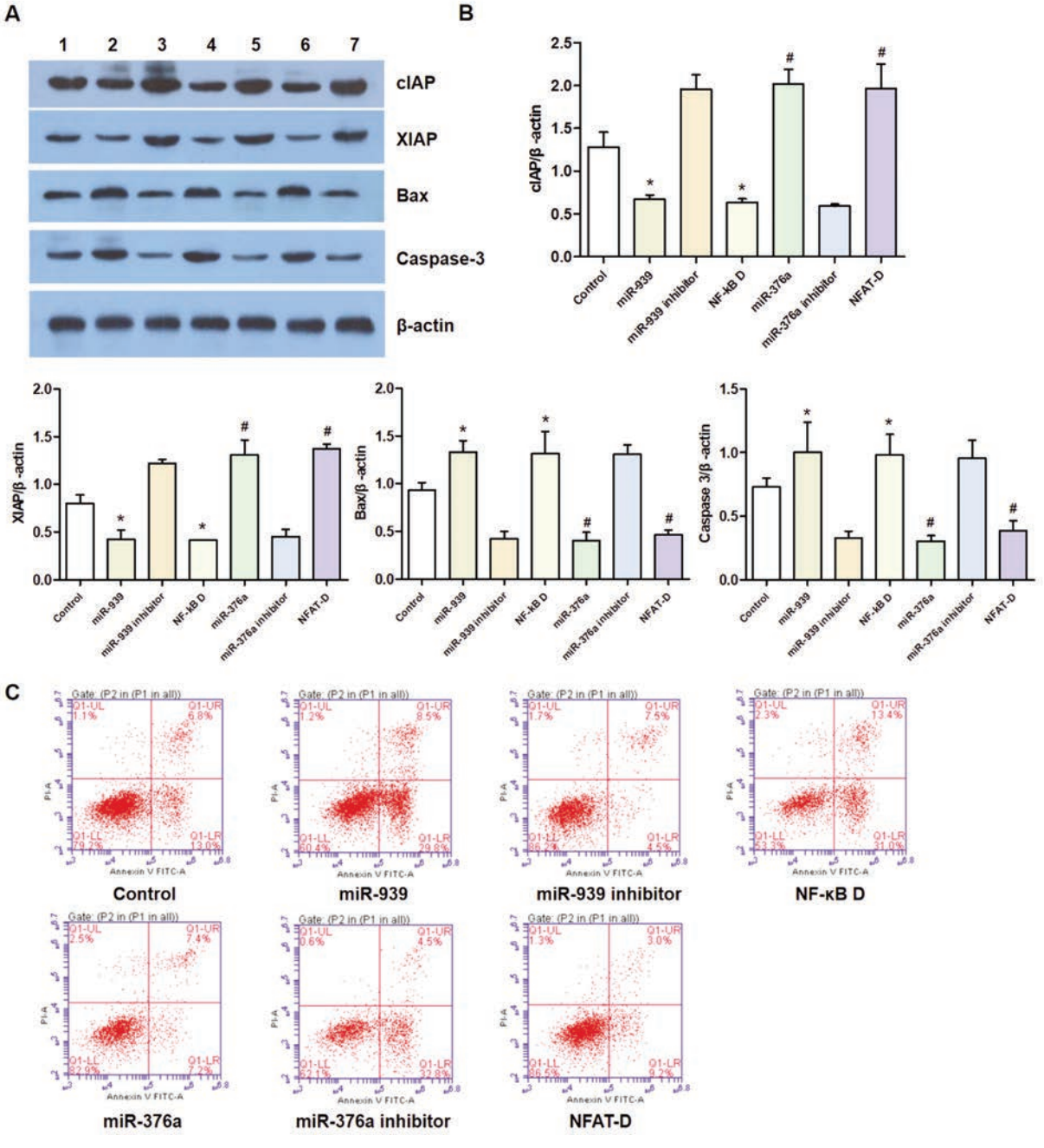

Figure 4. The inhibitory effect of trap strategy on intestinal epithelial cell apoptosis. A,B) The protein expression levels of cIAP, XIAP, Bax, and Caspase-3 was detected by Western blot. C) The transfected model cells were analyzed by flow cytometry; the dual parameter scatterplots is divided into four quadrants; the number of scatters in the lower right quadrant represents the number of apoptotic cells. Compared with control group, and miR-939 antisense oligonucleotide inhibitor group, *p<0.05; compared with control group, and miR-376a antisense oligonucleotide inhibitor group, #p<0.05.

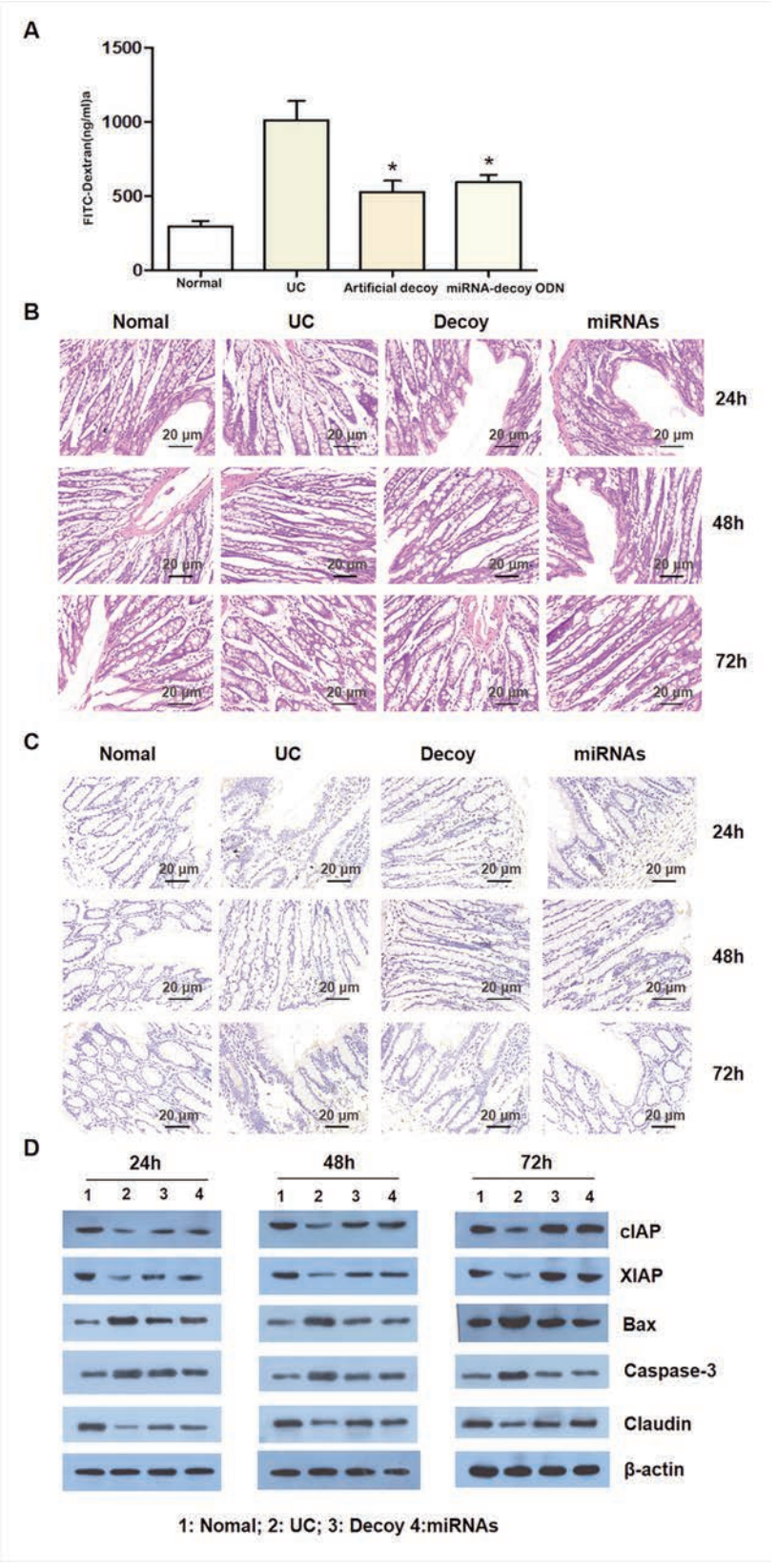

Figure 5. Therapeutic effects and side effects of decoy strategies on UC model mice. A) The permeability of intestinal cells was detected after transfection with different decoy molecules; the higher the detected fluorescence intensity, the higher the permeability of intestinal cells. B) At 24, 48 and 72 h after transfection, HE staining was used to observe the morphological changes of the colon tissues. C) At 24, 48 and 72 h after transfection, the expression of NF-κBp65 in colonic mucosal cells was observed by immunohistochemical staining. D) The protein expression levels of cIAP, XIAP, Bax, Caspase-3 and Claudin was detected at different transfection times by Western blotting. Compared with UC model group, *p<0.05.

of NF-κB and NFAT. The results of this study indicate that miR-939 and miR-376a act to trap NF-κB and NFAT, which inhibits the activation of the TFs NF-κB and NFAT, and subsequently inhibits the secretion of related inflammatory factors, playing an important role in the pathogenesis of UC.

Further study showed that compared with the controls, the tight junction proteins (Claudins, Occludins, and ZO-1) in the miR-939 group and ODN induced group was significantly increased, whereas the proportion of apoptosis was significantly decreased. miR-939 and miR-376a inhibited the activities of NF-κB and NFAT, and were beneficial to the inhibition of intestinal epithelial cell apoptosis, intestinal mucosal barrier, and repair and integrity in UC, and exerted an inhibitory effect on the pathogenesis and progression of UC. It has been reported that the inhibition of NF-κB and NFAT activity contributes to the improvement of inflammatory response, affecting the function of the intestinal mucosal immune system, and has therapeutic effects on inflammatory bowel disease.[28,29] The results of this study are consistent with previous studies.

Likewise, our animal experiments found that the disease activity index of the UC model group was significantly higher than that of the normal control group. The intestinal permeability in the artificially induced group and the miRNA-decoy ODN-transfected group was significantly lower than that in the UC model group, and the protein expression was significantly higher than that in the normal control group. The results of this study indicated that miR-939 and miR-376a could trap NF-κB and NFAT, and that the expression of miR-939 and miR-376a inhibited the activation of TFs NF-κB and NFAT, which had a therapeutic effect in the mouse model of UC.

In summary, the expression of miR-939 and miR-376A is reduced in tissues from patients with UC. The use of miR-939 and miR-376A to trap NF-κB and NFAT inhibits the activation of the TFs NF-κB and NFAT, and the expression of related inflammatory factors has a restorative effect on the intestinal barrier in UC. The decoy strategy inhibits apoptosis of the target cells and has a therapeutic effect in the mouse model of UC. This provides a new direction for the future development of clinical therapies for UC. However, this study still has some limitations. Under the decoy mechanism of miRNA, the research on the mice that established UC model is not in-depth enough. The feeding, mortality and time of death of mice cultured under different induction conditions can be counted, these statistical results can further assist to explain the therapeutic effect of the decoy mechanism on mice with UC. This research needs to be further studied.

References

1. Herrlinger K. Inflammatory bowel disease: an overview. Med Monatsschr Pharm 2013;36:402-8.
2. Eisenstein M. Ulcerative colitis: towards remission. Nature 2018;563:S33.
3. da Silva BC, Lyra AC, Rocha R, Santana GO. Epidemiology, demographic characteristics and prognostic predictors of ulcerative colitis. World J Gastroenterol 2014;20:9458-67.
4. Ng SC, Shi HY, Hamidi N, Underwood FE, Tang W, Benchimol EI, et al. Worldwide incidence and prevalence of inflammatory bowel disease in the 21st century: a systematic review of population-based studies. Lancet 2017;390:2769-78.
5. Ungaro R, Mehandru S, Allen PB, Peyrin-Biroulet L, Colombel JF. Ulcerative colitis. Lancet 2017;389:1756-70.
6. Yamamoto-Furusho JK, Gutiérrez-Grobe Y, López-Gómez JG, Bosques-Padilla F, Rocha-Ramírez JL, Grupo del Consenso Mexicano de Colitis Ulcerosa Crónica Idiopática. The Mexican consensus on the diagnosis and treatment of ulcerative colitis. Rev Gastroenterol Mex (Engl Ed) 2018;83:144-67.
7. Lan F, Yue X, Ren G, Li H, Ping L, Wang Y, et al. miR-15a/16 enhances radiation sensitivity of non-small cell lung cancer cells by targeting the TLR1/NF-κB signaling pathway. Int J Radiat Oncol Biol Phys 2015;91:73-81.
8. Zhou J, Ping FF, Lv WT, Feng JY, Shang J. Interleukin-18 directly protects cortical neurons by activating PI3K/AKT/NF-κB/CREB pathways. Cytokine 2014;69:29-38.
9. Yang HJ, Wang M, Wang L, Cheng BF, Lin XY, Feng ZW. NF-κB regulates caspase-4 expression and sensitizes neuroblas. toma cells to fas-induced apoptosis. PLoS One 2015;10:e0117953.
10. Goto T, Fukui A, Shibuya H, Keller R, Asashima M. Xenopus furry contributes to release of microRNA gene silencing. Proc Natl Acad Sci USA 2010;107:19344-9.
11. McKenna LB, Schug J, Vourekas A, McKenna JB, Bramswig NC, Friedman JR, et al. MicroRNAs control intestinal epithelial differentiation, architecture, and barrier function. Gastroenterology 2010;139:1654-64.
12. Ahmad MZ, Akhter S, Mallik N, Anwar M, Tabassum W, Ahmad FJ. Application of decoy oligonucleotides as novel therapeutic strategy: a contemporary overview. Curr Drug Discov Technol 2013;10:71-84.
13. Remes A, Wagner AH, Schmiedel N, Heckmann M, Ruf T, Ding L, et al. AAV-mediated expression of NFAT decoy oligonucleotides protects from cardiac hypertrophy and heart failure. Basic Res Cardiol 2021;116:38.
14. Kim KH, Park JH, Lee WR, Park JS, Kim HC, Park KK. The inhibitory effect of chimeric decoy oligodeoxynucleotide against NF-κB and Sp1 in renal interstitial fibrosis. J Mol Med (Berl) 2013;91:573-86.
15. Correia de Sousa M, Gjorgjieva M, Dolicka D, Sobolewski C, Foti M. Deciphering miRNAs' Action through miRNA Editing. Int J Mol Sci 2019;20:6249.
16. Chunhui C, Jinlong Y, Shuxin H, Huiquan Z, Zonghai H. transcriptional regulation of gene expression by microRNAs as endogenous decoys of transcription factors. Cell Physiol Biochemistry 2014;33:1698-14.
17. Atreya I, Atreya R, Neurath MF. NF-kappaB in inflammatory bowel disease. J Intern Med 2008;263:591-6.
18. Chand S, Mehta N, Bahia MS, Dixit A, Silakari O. Protein kinase C-theta inhibitors: a novel therapy for inflammatory disorders. Curr Pharm Des 2012;18:4725-46.
19. Kornbluth A, Sachar DB, Practice Parameters Committee of the American College of Gastroenterology. Ulcerative colitis practice guidelines in adults (update): American College of Gastroenterology, Practice Parameters Committee. Am J Gastroenterol 2004;99:1371-85. Erratum in Am J Gastroenterol 2010;105:500.
20. Wang YF, Ouyang Q, Hu RW. Progression of inflammatory bowel disease in China. J Dig Dis 2010;11:76-82.
21. Li L, Miao X, Ni R, Miao X, Wang L, Gu X, et al. Epithelial-specific ETS-1 (ESE1/ELF3) regulates apoptosis of intestinal epithelial cells in ulcerative colitis via accelerating NF-κB activation. Immunol Res 2015;62:198-212.
22. Matricon J, Barnich N, Ardid D. Immunopathogenesis of inflammatory bowel disease. Self Nonself 2010;1:299-309.
23. Mennigen R, Nolte K, Rijcken E. Probiotic mixture VSL3 protects the epithelial barrier by maintaining tight junction protein expression and preventing apoptosis in a murine model of colitis. Am J Physiol Gastrointest Liver Physiol 2009;296:G1140-9.
24. Oshima T, Miwa H, Joh T. Changes in the expression of claudins in active ulcerative colitis. J Gastroenterol Hepatol 2008;23:S146-50.

25. Jacknowitz AI. Ulcerative colitis and its treatment. Am J Hosp Pharm 1980;37:1635-46.
26. Tang P, Xiong Q, Ge W, Zhang L. The role of microRNAs in osteoclasts and osteoporosis. RNA Biol 2014;11:1355-63.
27. Rencz F, Péntek M, Bortlik M, Zagorowicz E, Hlavaty T, Śliwczyński A, et al. Biological therapy in inflammatory bowel diseases: Access in Central and Eastern Europe. World J Gastroenterol 2015;21:1728-37.
28. Atreya I, Atreya R, Neurath MF. NF-kappaB in inflammatory bowel disease. J Intern Med 2008;263:591-6.
29. Vora P, McGovern DP. LRRK2 as a negative regulator of NFAT: implications for the pathogenesis of inflammatory bowel disease. Expert Rev Clin Immunol 2012;8:227-9.

Received for publication: 8 August 2021. Accepted for publication: 9 December 2021.

European Journal of Histochemistry 2022; 66:3316
doi:10.4081/ejh.2022.3316